

Nano- and Microscopic Surface Wrinkles of Linearly Increasing Heights Prepared by Periodic Precipitation

Stoyan K. Smoukov, Agnieszka Bitner, Christopher J. Campbell, Kristiana Kandere-Grzybowska, and Bartosz A. Grzybowski*

Contribution from the Department of Chemical and Biological Engineering and The Northwestern Institute on Complex Systems, Northwestern University, 2145 Sheridan Road, Evanston, Illinois 60208

Received July 21, 2005; E-mail: grzybor@northwestern.edu

Abstract: Arrays of surface wrinkles of linearly increasing heights (from tens of nanometers to tens of micrometers) were prepared via a spontaneous reaction–diffusion process based on periodic precipitation. The slopes, dimensions, and positions of the precipitation bands could be controlled precisely by adjusting the concentrations of the participating chemicals as well as the material properties of patterned substrates. Additional control of periodic precipitation by localized UV irradiation allowed for the preparation of discontinuous and curvilinear structures. The nonbinary 3D surface topographies were replicated into poly(dimethylsiloxane), and the applications of replicas in microfluidics, microseparations, and cell biology have been suggested.

Introduction

The ability to decorate surfaces with nonbinary reliefs—that is, reliefs whose protrusions vary in heights—is sought in microfluidics,¹ microoptics,^{2,3} and tissue/cellular engineering.⁴ The existing methods for multilevel surface structuring are either serial in nature (e-beam,⁵ Focused Ion Beam (FIB),⁵ micro-stereolithography⁶) or require multiple registration steps; in addition, the control of features' heights with sub-micrometer precision remains a challenging task requiring highly specialized equipment (e.g., Reactive Ion Etching (RIE)-lag,⁷ Hole Area Modulation (HAM),⁸ and focused electron beam⁹). We have recently suggested^{10–14} that self-organization based on spontaneous chemical processes^{15,16} can provide a flexible basis for

creating three-dimensional surface reliefs. Our strategy has been to “program” the fabrication process using chemical reactions occurring in soft media in such a way that the amount of a reaction product created at a given location would translate into surface elevation therein. We have applied this strategy successfully to create surface microtopographies with uses in microfluidic¹⁰ and optical devices.^{11,14} Here, we show how self-organization based on periodic precipitation (PP)^{17–19}—that is, a phenomenon in which inorganic salts diffusing through a gel form mobile colloidal precipitates that subsequently aggregate into well-defined and regularly spaced precipitation bands—can be used to prepare nanostructured and microstructured substrates having regular undulations of linearly increasing heights (from tens-of-nanometers to tens of micrometers; Figures 1–3). The slopes and dimensions of these structures and the loci at which they form can be controlled by adjusting the concentrations of the participating chemicals and by the material properties of the substrate. The nanowrinkled surfaces are useful constructs with which to study wetting phenomena and cell orientations on topographical gradients.

Experimental Section

(i) In the general procedure, PP was initiated in a thin layer of ionically doped gel using the wet stamping (WETS) technique described in detail elsewhere^{15,18,20} (Figure 1a). An agarose block was soaked in

- (1) Toepke, M. W.; Kenis, J. A. *J. Am. Chem. Soc.* **2005**, *127*, 7674–7675.
- (2) Quake, S. R.; Scherer, A. *Science* **2000**, *290*, 1536–1540.
- (3) Golub, M. A.; Friesem, A. A.; Eisen, L. *Opt. Commun.* **2004**, *235*, 261–267.
- (4) Flemming, R. G.; Murphy, C. J.; Abrams, G. A.; Goodman, S. L.; Nealey, P. F. *Biomaterials* **1999**, *20*, 573–588.
- (5) Clough, R. L. *Nucl. Instrum. Methods Phys. Res., Sect. B* **2001**, *185*, 8–33.
- (6) Zhang, X.; Jiang, X. N.; Sun, C. *Sens. Actuator, A* **1999**, *77*, 149–156.
- (7) Chung, C. K. *J. Micromech. Microeng.* **2004**, *14*, 656–662.
- (8) Masuzawa, T.; Olde-Benneker, J.; Eindhoven, J. J. C. *Ann. CIRP* **2000**, *49*, 139.
- (9) Gates, B. D.; Whitesides, G. M. *J. Am. Chem. Soc.* **2003**, *125*, 14986–14987.
- (10) Campbell, C. J.; Klajn, R.; Fialkowski, M.; Grzybowski, B. A. *Langmuir* **2005**, *21*, 418–423.
- (11) Campbell, C. J.; Baker, E.; Fialkowski, M.; Grzybowski, B. A. *Appl. Phys. Lett.* **2004**, *85*, 1871–1873.
- (12) Smoukov, S. K.; Bishop, K. J. M.; Campbell, C. J.; Grzybowski, B. A. *Adv. Mater.* **2005**, *17*, 751–755.
- (13) Grzybowski, B. A.; Bishop, K. J. M.; Campbell, C. J.; Fialkowski, M.; Smoukov, S. *Soft Matter* **2005**, *1*, 114–128.
- (14) Campbell, C. J.; Baker, E.; Fialkowski, M.; Bitner, A.; Smoukov, S. K.; Grzybowski, B. A. *J. Appl. Phys.* **2005**, *97*, Article #126102.
- (15) Campbell, C. J.; Fialkowski, M.; Klajn, R.; Bensemann, I. T.; Grzybowski, B. A. *Adv. Mater.* **2004**, *16*, 1912–1917.
- (16) Klajn, R.; Fialkowski, M.; Bensemann, I. T.; Bitner, A.; Campbell, C. J.; Bishop, K.; Smoukov, S.; Grzybowski, B. A. *Nat. Mater.* **2004**, *3*, 729–735.

- (17) (a) Liesegang, R. E. *Naturwiss. Wochenschr.* **1896**, *11*, 353, 1.1, 5.1. (b) Heinsch, H. K. In *Crystals in Gels and Liesegang Rings*; Cambridge University Press: Cambridge, U.K., 1988; Ch. 5.
- (18) Bensemann, I. T.; Fialkowski, M.; Grzybowski, B. A. *J. Phys. Chem. B* **2005**, *109*, 2774–2778.
- (19) (a) Muller, S. C.; Ross, J. *J. Phys. Chem. A* **2003**, *107*, 7997–8008. (b) Fialkowski, M.; Bitner, A.; Grzybowski, B. A. *Phys. Rev. Lett.* **2005**, *94*, 018303. (c) LeVan, M. E.; Ross, J. *J. Phys. Chem.* **1987**, *91*, 6300–6308. (d) Avnir, D.; Kagan, M. *Nature* **1984**, *307*, 717–720. (e) Jablczynski, C. K. *Bull. Soc. Chim. Fr.* **1923**, *33*, 1592–1602. (f) Racz, Z. *Physica A* **1999**, *274*, 50–59. (g) Krug, H.-J.; Brandtstadter, H. *J. Phys. Chem. A* **1999**, *103*, 7811–7820.

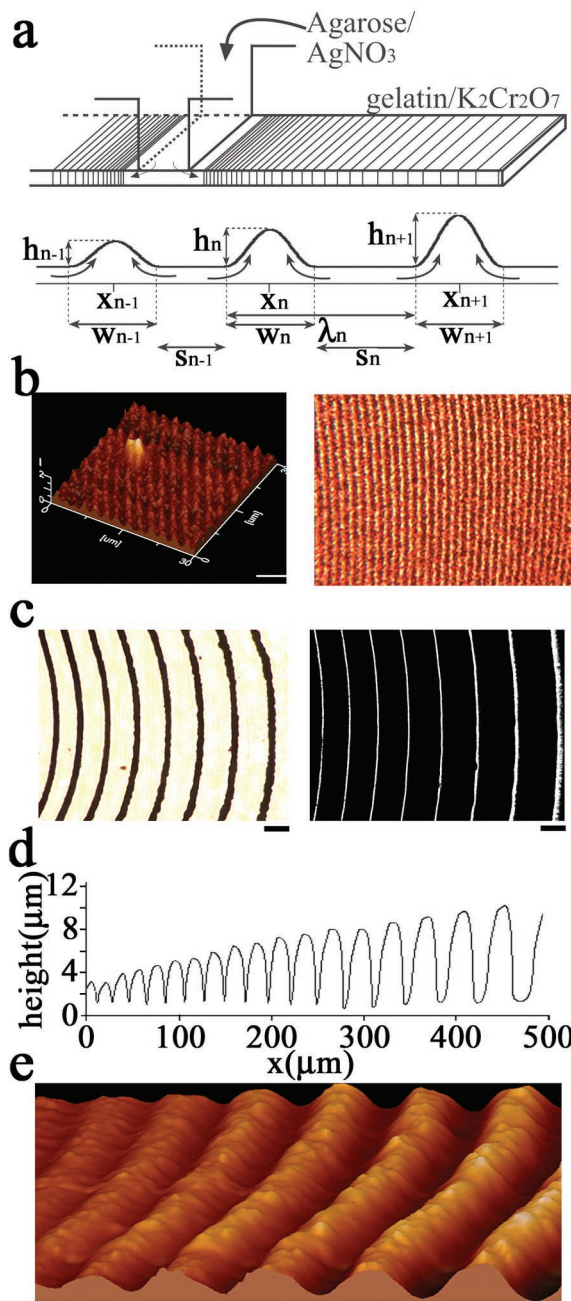


Figure 1. Arrays of nano- and microscopic surface wrinkles obtained by periodic precipitation. The scheme in a illustrates the experimental arrangement and defines pertinent dimensions. b Atomic force microscopy (AFM) scan (left) and an optical micrograph (right) of parallel PP bands characterized by $\lambda = 1.4 \mu\text{m}$. (c) The relative width of the dark bands and clear slits is the function of the concentrations of reacting salts. Scale bars are 50 and 20 μm , respectively. (d) Profilogram and an AFM scan of a PDMS replica of a gelatin film decorated with wrinkles of linearly increasing heights (25% AgNO_3 , 10% $\text{K}_2\text{Cr}_2\text{O}_7$, $E = 0 \text{ mJ/cm}^2$). (e) The AFM resolves the first few bands whose heights increase smoothly from 200 nm to $\sim 2 \mu\text{m}$. The scale bar below the AFM is 10 μm .

a 20–50% AgNO_3 solution, dried by placing on a filter paper for up to 1 h, and finally applied onto a thin layer of dry gelatin doped with 5–25% of $\text{K}_2\text{Cr}_2\text{O}_7$ (throughout the paper, all concentrations are w/w). Prior to use, the degree of gelatin cross-linking^{21,22} was controlled by

- (20) Fialkowski, M.; Campbell, C. J.; Bensemann, I. T.; Grzybowski, B. A., *Langmuir* **2004**, *20*, 3513–3516.
 (21) Li, H.; Huang, X. Mechanism of Enzyme-Etching Dichromated Gelatin and Swelling of Gelatin. In *Micromachining and Microfabrication Process Technology*, 7th ed.; Karam, J. M., Yasaitis, J., Ed.; SPIE: Bellingham, WA, 2001.

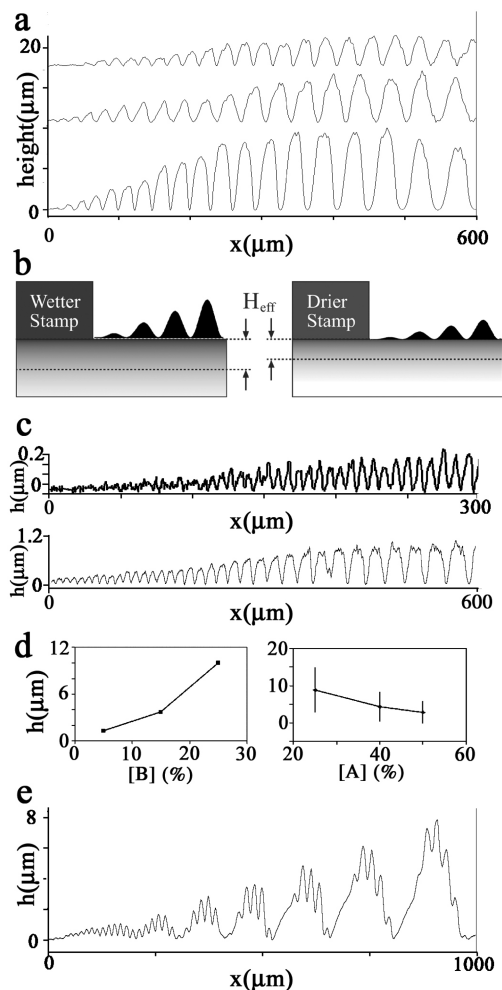


Figure 2. Profilograms of wrinkled surfaces. (a) Profilogram of PP bands for various times of stamp drying, t_{dry} : 4 h (top profile), 1 h (middle), and 20 min (bottom). (b) Illustration of the effective hydrated layer. (c) The heights and slopes of the wrinkles decrease with increasing irradiation time: $E = 180 \text{ mJ/cm}^2$ for the top profile; $E = 11 \text{ mJ/cm}^2$ for the bottom one (4.5 μm gels, 12% $\text{K}_2\text{Cr}_2\text{O}_7$, 45% AgNO_3 , $t_{\text{dry}} = 1 \text{ h}$). (d) Wrinkle heights, h , increase with increasing $[\text{K}_2\text{Cr}_2\text{O}_7]$ (left graph) and decrease when $[\text{AgNO}_3]$ increases (right graph); the trends were obtained by comparing the heights of precipitation bands of the same number $n = 20$ on gels differing only in the concentration of either $\text{K}_2\text{Cr}_2\text{O}_7$ or AgNO_3 . Standard deviations were taken from three to five independent experiments. (e) Profilogram of a complex surface topography with two periodicities.³⁰

exposing its entire surface (or only parts of it, using a photomask) to ultraviolet radiation (365 nm, 18 mW/cm^2) for varying exposures, $E = 10\text{--}6500 \text{ mJ/cm}^2$.

(ii) The dependence of the surface wrinkles' slopes on the water content in the stamp was studied using un-irradiated, 20 μm thick gels doped with 20% $\text{K}_2\text{Cr}_2\text{O}_7$ and stamps soaked in 25% AgNO_3 solution. Prior to the formation of PP patterns, all stamps were first dried on a filter paper for 20 min and then kept on an absorptive dry gelatin film for $t_{\text{dry}} = 20 \text{ min}$ to $t_{\text{dry}} = 4 \text{ h}$ (Figure 2a).

(iii) Poly(dimethylsiloxane) (PDMS) replicas were prepared by casting a 10:1 (w/w), degassed mixture of PDMS prepolymer and curing agent (Sylgard 184; Dow) against PP arrays developed in gelatin. The elastomer was cured overnight in the dark and at room temperature and was then gently peeled off the gelatin master.

(iv) Dewetting experiments were performed using PDMS replicas of an array of parallel wrinkles increasing linearly in heights from 4 to

- (22) Manivannan, G.; Changkakoti, R.; Lessard, R. A.; Mailhot, G.; Bolte, M. M., *J. Phys. Chem.* **1993**, *97*, 7228–7233.

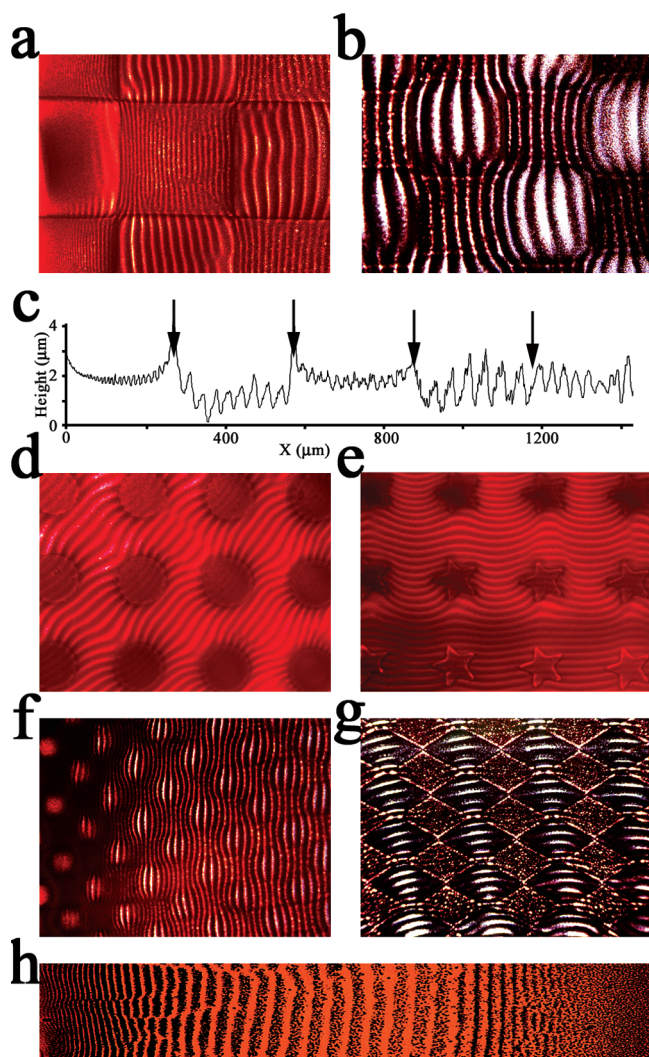


Figure 3. Periodic precipitation structures on photopatterned gels. (a) UV exposure 810 mJ/cm². Panel c is a profile of a. (b and d–f) UV exposure 300 mJ/cm². (g) UV exposure > 1500 mJ/cm². (h) PP pattern exhibiting both positive and negative values of the spacing coefficient, p . The left half of the pattern developed for 2 h in the dark; the right half, in the light for 4 h afterward.

8 μm . These replicas were pulled out of either a light mineral oil (Fisher Scientific, Fair Lawn, NJ) or pure ethylene glycol at a speed of 7.5 cm/h using a syringe pump. Wetting angles of both liquids on oxidized PDMS were measured using a Rame-Hart 100 goniometer and were $26.6 \pm 2.0^\circ$ for oil and $87.6 \pm 2.8^\circ$ for ethylene glycol.

Results and Discussion

When silver nitrate diffused from the applied agarose stamp into the dry gelatin film, it reacted with potassium dichromate contained therein to give a deep-brown precipitate of silver dichromate. Subsequently, this precipitate aggregated into an immobile phase collected in distinct bands of periodic precipitation whose formation was governed by a complex reaction–diffusion–aggregation mechanism,^{18,19} and whose *relative* positions x_n increased in a geometrical proportion according to $x_{n+1} = (1 + p)x_n$ with the spacing coefficient, p , dependent on the geometrical parameters of the system (we note that the absolute spacing λ between consecutive waves is not related to p).

Resolution of micro- and nanoscale bands was achieved by minimizing hydrodynamic effects accompanying the transfer of AgNO₃ into gelatin. We have previously shown¹⁸ that these

effects suppressed the formation of distinct PP bands and gave rise to a uniform transient precipitation zone extending a couple of hundred of micrometers from the source of the outer electrolyte—as a result, the first resolved bands had minimal thickness in the tens of micrometers. In this study, the combination of gel cross-linking using UV and the dehydration (i.e., drying) of agarose blocks prior to stamping slowed the water transport, rendered the delivery of AgNO₃ purely diffusive, and allowed resolution of large numbers (up to 100) of smooth bands as thin as 700 nm and of minimal height \sim 20 nm.

Both horizontal and vertical dimensions (cf. Figure 1a) of the PP bands depended on the initial concentrations of chemicals used and on the degree of gel cross-linking. The values of λ decreased with increasing cross-linking due to lowering of the nucleation/aggregation thresholds in “denser” gels and to slower diffusion of the species involved.¹⁸ In addition, λ decreased with increasing concentration of AgNO₃ which reduced the difference between osmotic pressures in the stamp and in the dry gel,²⁰ and led to lower gel hydration and lower nucleation threshold. Band separations as small as $\lambda = 1.4 \mu\text{m}$ ($w = s = 700 \text{ nm}$) were resolved with [AgNO₃] = 60%, [K₂Cr₂O₇] = 20%, and $E \sim 6000 \text{ mJ/cm}^2$ (Figure 1b). Finally, the relative widths of the bands (i.e., the ratios w/λ) increased with increasing concentration of AgNO₃ and varied between 0.2 when the concentrations of both salts were low (10% AgNO₃, 10% K₂Cr₂O₇, $w_{\text{min}} = 16 \mu\text{m}$; Figure 1c, left) to 0.95 when 25% AgNO₃ and 25% K₂Cr₂O₇ were used (Figure 1c, right; $s_{\text{min}} = 900 \text{ nm}$)—this trend is explained by the Matalon–Packter law²¹ and the observation¹⁶ that w increases only very slowly compared to λ .

The heights of the successive bands increased linearly with band location (Figure 1d; Figure 2) over distances up to \sim 1 mm over which the gel was hydrated. This was because (i) all Ag₂Cr₂O₇ produced was collected in the bands, (ii) the amount of Ag₂Cr₂O₇ collected by each band was proportional to its position, x_n , and (iii) the deformation of the substrate was linearly proportional to the amount of precipitate at a given location.¹⁸ Importantly, the heights h_n of the bands and/or the slopes $WS = (h_n/x_n)$ of the height increase could be modulated by varying the degree of substrate hydration, concentration of inner and outer electrolytes, and/or the degree of substrate cross-linking; for thin gels we used (4–20 μm), thickness had negligible effect on the values of h_n and WS . In the following, we discuss how each of these parameters affects surface topography assuming that all other experimental variables are kept constant:

(1) Degree of Hydration. The slopes of the wrinkle arrays increase with an increasing amount of water delivered into the gelatin (Figure 2a). Wetter stamps (Figure 2b, left) hydrate the gel to a higher effective depth,^{18,20} H_{eff} , than drier ones (Figure 2b, right), allowing periodic precipitation to occur in a thicker layer. Since the amount of precipitate produced (per unit area of the surface) scales with this layer’s thickness, so does the degree of the gelatin deformation along the precipitation bands. The wetter the gelatin, the higher are the PP bands. Furthermore, because the positions of the bands depend only weakly on the water content, the slopes, WS , increase with the degree of substrate hydration.

(2) Degree of Cross-Linking. UV irradiation causes gel cross-linking via reduction of chromate ions.^{21,22} As a result,

the amount of the inner (i.e., dichromate) electrolyte decreases while the gel becomes stiffer (i.e., harder to buckle)—both of these effects reduce the heights of the surface undulations. This reduction is more pronounced than the concomitant decrease in λ , and overall the slopes decrease with increasing irradiation time (Figure 2c).

(3) Concentration of $K_2Cr_2O_7$. Because potassium dichromate is the limiting reagent for the PP process, its concentration in the substrate determines the total amount of precipitate produced and collected into the bands. It follows that the bands' heights increase with increasing $[K_2Cr_2O_7]$ (comparisons made for the bands of the same number, $n = 20$; Figure 2d, left). At the same time, the spacing between the bands decreases with increasing concentration of dichromate¹⁷ (Matalon–Packter law²³), so WS can either increase or decrease depending on the relative magnitudes of these two opposing effects.

(4) Concentration of $AgNO_3$. An increase in concentration of the outer electrolyte does not affect the total amount of precipitate (limited by $[K_2Cr_2O_7]$) but reduces the spacing between the bands—consequently, the number of bands per unit length increases, and their heights decrease (comparison for $n = 20$; Figure 2d, right). The slopes can either decrease or increase depending on the value of $[AgNO_3]$.

We note that although the degree of hydration and cross-linking were quantified only in terms of process variables (drying time, exposure), the control of all four variables was adequate to reproduce the band heights and slopes to within 20% between experiments.

Combination of periodic precipitation and spatially selective photopatterning can produce nanostructured surfaces on which the PP bands do not necessarily grow monotonically and need not be continuous. Figure 3a shows an example of a surface irradiated with UV light ($E = 810 \text{ mJ/cm}^2$) through a chessboard transparency mask. The structures forming on irradiated regions are thinner than those on unirradiated ones, and the junctions between bands on different squares are discontinuous. The surface profile in Figure 3c shows that the corresponding nanotopographies alternate between low (irradiated regions) and high (unirradiated regions) amplitudes. When the irradiation times are shorter and the “contrast” between the degree of cross-linking is lower ($E = 300 \text{ mJ/cm}^2$), bands on different regions are commensurate in thickness, and instead of breaking, they curve to maintain continuity (Figure 3b,d–f). On the other hand, in the regime of very long irradiation times, the exposed regions do not support PP at all, and surface wrinkles form only on disjoint, unirradiated portions of the gel ($E > 1500 \text{ mJ/cm}^2$; Figure 3g). Finally, when PP patterns are developed while irradiating the gel, the values of the spacing coefficient, p , can be varied in real time by increasing the UV exposure. This effect is vividly illustrated in Figure 3h in which a steady increase in UV exposure produced a pattern characterized by both positive (left, unirradiated portion) and negative (right portion) values of p (this system is effectively a chemical actinometer²⁴ with visual pattern readout).

Patterned gels can be easily replicated into polymeric materials without destruction of the nanotopography developed by periodic precipitation. PDMS replicas (Figures 1d and 4) of

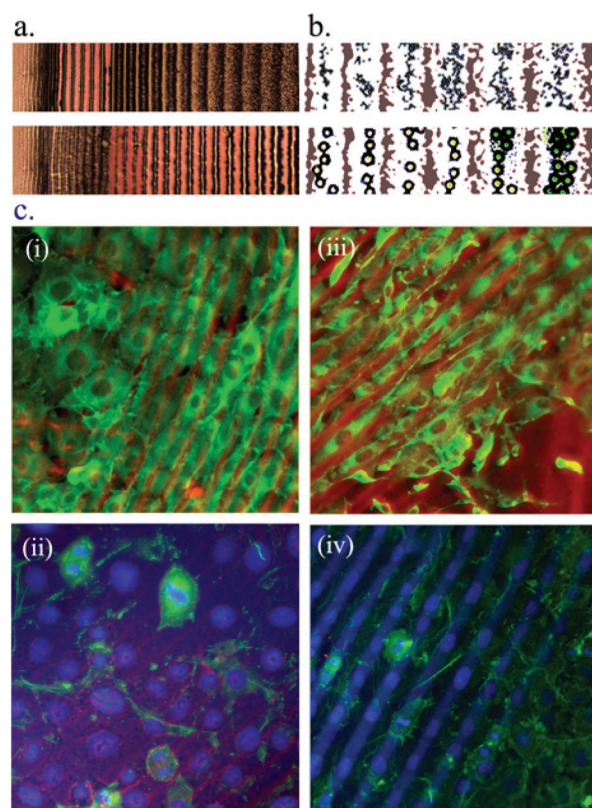


Figure 4. (a) Discontinuous dewetting of light mineral oil (top) and pure ethylene glycol (bottom) from an oxidized PDMS replica of an array of parallel undulations, whose heights increase linearly from 4 (left) to 8 μm (right). Color of both liquids was adjusted electronically for clarity. (b) The same PDMS replica allowed capturing microspheres of diameters up to a critical value of $\sim 20 \mu\text{m}$ from a 1:1 (v/v) mixture of EG and distilled water (top picture, 5.7 μm spheres; bottom picture, 15 μm ; crests of the PP bands are colored brown). (c) Organization of Rat2 fibroblast cells on wrinkle arrays of heights increasing linearly from $\sim 200 \text{ nm}$ (i, ii) to $\sim 10 \mu\text{m}$ (iii, iv).

the wrinkle arrays have proven useful in several basic studies and potential applications. For example, in Figure 4a these structures were used as substrates for discontinuous dewetting.²⁵ This method can be used for estimation of wetting angles of various liquids: liquids characterized by low angles (with respect to the substrate material) fill high-curvature spaces between small wrinkles, while those of high angles fill low-curvature, large ones only.^{26,27} The wrinkle arrays are also interesting in the context of positioning/sorting small particles. When solutions of small latex spheres were flushed over such surfaces from the direction of the smallest surface undulations, the wrinkles captured only the spheres of diameters below a certain threshold value (e.g., $\sim 20 \mu\text{m}$ for the structure shown in Figure 4b). In addition, particles that were captured were deposited with a gradient of surface density—fewer between smaller wrinkles and more between larger ones. Finally, our nanostructured substrata are interesting constructs with which to study and/or control cellular orientation, differentiation, and functionality—an ability sought in tissue/cellular engineering and developmental cell biology.^{4,28,29} In contrast to surface reliefs

(25) Jackman, R. J.; Duffy, D. C.; Ostuni, E.; Willmore, N. D.; Whitesides, G. M. *Anal. Chem.* **1998**, *70*, 2280–2287.

(26) Netz, R. R.; Andelman, D. *Phys. Rev. E* **1997**, *55*, 687–693.

(27) Seemann, R.; Brinkmann, M.; Kramer, E. J.; Lange, F. F.; Lipowsky, R. *Proc. Natl. Acad. Sci. U.S.A.* **2005**, *102*, 1848–1852.

(28) Curtis, A.; Wilkinson, C. *Trends Biotechnol.* **2001**, *19*, 97–101.

(29) Andersson, H.; van den Berg, A. *Lab Chip* **2004**, *4*, 98–103.

(23) Matalon, R.; Packter, A. *J. Colloid. Sci.* **1955**, *10*, 46.

(24) Kuhn, H. J.; Braslavsky, S. E.; Schmidt, R. *Pure Appl. Chem.* **2004**, *76*, 2105–2146.

having binary topographies, the “wavy” supports of varying heights allow parallel (i.e., simultaneous) monitoring of cellular responses to a continuum of surface topographies. This is illustrated in Figure 4c, which shows organization of Rat2 fibroblast cells on patterns growing linearly in height from ~ 20 nm to $\sim 10 \mu\text{m}$. Pictures in the left column show cells on the region of the wrinkles where the heights increase from ~ 200 to 400 nm, and spacing is approximately $10 \mu\text{m}$. Picture i is a superposition of a phase-contrast image showing the presence of surface structures (red channel) and fluorescence image visualizing cell shape by actin staining with phalloidin-Alexa 488 (green channel). As the wrinkles’ heights increase (from upper left to lower right in all pictures), cells progressively orient in the grooves between them. Picture ii merges three channels—DNA staining with 4',6-diamidino-2-phenylindole (DAPI) to visualize nuclei (blue), actin staining with phalloidin-Alexa488 (green), and phase-contrast to visualize the surface (red). As seen, small wrinkles do not influence the shapes of the nuclei, which remain roughly circular. In contrast, cells on larger undulations—in pictures iii and iv spaced by $30\text{--}40$ and $\sim 10 \mu\text{m}$ high—are fully oriented along the grooves; interestingly,

(30) While we do not understand the origin of such secondary precipitation structures superimposed on the primary waves, we have established that they appear in highly hydrated and unirradiated gels when the concentration of outer electrolyte is significantly higher than that of the inner one (here, $[\text{AgNO}_3] = 15\text{--}25\%$; $[\text{K}_2\text{Cr}_2\text{O}_7] = 5\%$). For discussion, see: (a) Holba, V.; Fusek, F. *Collect. Czech. Chem. Commun.* **2000**, *65*, 1438–1442. (b) Holba, V. *Colloid Polym. Sci.* **1989**, *267*, 456–459. (c) Hantz, P. *Phys. Chem. Chem. Phys.* **2002**, *4*, 1262–1267.

their nuclei are also elongated in this direction. More work is needed to quantify these preliminary results.

Conclusions

In summary, we have developed and rationalized a simple and flexible method for decorating surfaces with regular arrays of nano- and microscopic surface wrinkles of increasing heights. On the fundamental level, this work confirms that chemical self-organization can be an efficient way of preparing small-scale architectures that would be hard to fabricate by conventional means. We believe the wavy nanotopographies will be useful as test beds for studying friction and wetting at small scales, as diffractive optical elements, and as substrates for studying/promoting cellular motility on patterned surfaces.

Acknowledgment. We would like to thank Dr. Marcin Fialkowski for helpful discussions on periodic precipitation patterns. B.A.G. gratefully acknowledges financial support from the Camille and Henry Dreyfus New Faculty Awards Program and the National Science Foundation (Grant No. 0503673) A.B. was supported by a postdoctoral fellowship from the Northwestern Institute of Complexity. C.J.C. was supported in part by the NSF-IGERT program “Dynamics of Complex Systems in Science and Engineering” (Grant DGE-9987577). K.K.-G. is a postdoctoral DOD Fellow.

JA054882J